

KONDO / HEAVY FERMION SYSTEMS

High Field ^{11}B NMR Study of the Mixed Valent Compound SmB_6 and La Doped CaB_6

NHMFL

Abdelrazek, M.M., NHMFL
Caldwell, T., NHMFL
Reyes, A.P., NHMFL
Kuhns, P.L., NHMFL
Moulton, W.G., NHMFL
Achey, R.M., NHMFL
Young, D.P., NHMFL
Fisk, Z., NHMFL

There is strong evidence that SmB_6 is a small gap semiconductor, and a mixed valence system. The

Sm^{2+} configuration is non-magnetic while the Sm^{3+} configuration should be magnetic. The cubic structure of the hexaborides has only one site for the Sm ion. Low field ($H_0 = 1.5$ T) NMR measurements on SmB_6 have been done previously by Takigawa.¹ A gapped density of states was used to explain the temperature dependence of $1/T_1$ above 20 K. The ^{11}B spectrum for $\text{Ho} \parallel [001]$ in SmB_6 was observed at a range of high fields (5 T and above) from 4 K to 300 K as shown in Figure 1.

In the hexaboride structure, the magnetic field divides the six crystallographically-equivalent boron sites into two magnetically nonequivalent sites; two apical (parallel to the field) B_1 , and four planar (perpendicular to the field) B_2 . Thus for the applied field parallel to the $[001]$ direction (along the apical axis), and if there were no shift

anisotropy and $\eta=0$ (by symmetry), five equally spaced lines should be seen. The B_1 peak is shifted to higher field, thus separating it from the B_2 sites, resulting in two sets of quadrupole split lines. In addition, there is a B-B nuclear dipole splitting of 12G of the B_1 lines. The paramagnetic shift is -0.06% for $\theta=0^\circ$ and 0.01% for $\theta=90^\circ$ in SmB_6 from these data, and is independent of temperature and field. This paramagnetic shift of B_1 borons from the B_2 borons is absent in the $\text{Ca}_{0.995}\text{La}_{0.005}\text{B}_6$, with the center at the unshifted γ for ^{11}B . The dipolar splitting is present in the satellites. The independence of the splitting of the apical B sites from the planar sites suggests there is no evidence for a localized moment on the Sm^{3+} contribution to the mixed valence state in SmB_6 , and the absence of the shift in $\text{Ca}_{0.995}\text{La}_{0.005}\text{B}_6$ indicates the shift is due to the orbital contribution from the Sm. The T_1 data as a function of temperature appears to follow the carrier concentration and shows typical gap behavior above 20 K with a “kink” below 20 K.

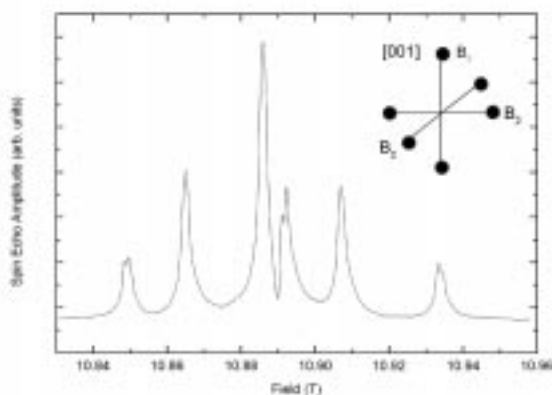


Figure 1. Field swept ^{11}B NMR spectrum for SmB_6 at 4 K.

This research is supported by the NHMFL In-House Research Program.

Reference:

- 1 Takigawa, M., *et al*, J. Phys. Soc. Jap., **50**, 2525 (1981).

High Field Transport in the Rare Earth Hexaborides

Aronson, M.C., Univ. of Michigan, Physics
 Bogdanovich, S., Univ. of Michigan, Physics
 Fisk, Z., NHMFL
 Tozer, S.W., NHMFL

This year we continued our research program on the magnetism of rare earth hexaborides with two different high field experiments. The first was a study of the magnetoresistance and magnetization of high quality single crystals of EuB_6 , for temperatures from 1.2 K to 25 K, and fields as large as 30 T. Examples of our results are shown in Figure 1. Shubnikov-de Haas and de Haas-van Alphen oscillations were observed with four distinct fundamental frequencies, indicating that the Fermi surface consists of separate pockets for electrons and holes. The effective masses and extremal areas for the pockets are in good agreement with those predicted by recent band structure calculations. This work comprises the first direct experimental evidence that EuB_6 is an intrinsic semimetal, not

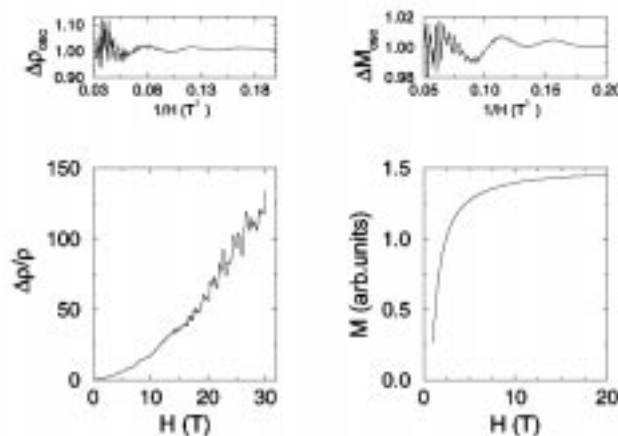


Figure 1. (lower left) The magnetoresistance of EuB_6 at 0.4 K. Field is along 001 axis, and current flows approximately along the 100 axis. (upper left) The oscillatory part of the magnetoresistance as a function of inverse field. (lower right) The magnetic torque of EuB_6 at 4.3 K, with the field parallel to the 001 axis. (upper right) The oscillatory part of the magnetization as a function of inverse field.

a doped insulator, as has been historically assumed. We find no appreciable modification to the Fermi surface dimensions or carrier masses with the onset of ferromagnetism, in contrast to a zero field light scattering study which claimed that ferromagnetic order is accompanied by the formation of magnetic polarons.

The goal of our second experiment was to study the metallization of the mixed valence compound SmB_6 which we previously observed at 60 kbar. We wished to search for low temperature instabilities in the gapless metallic phase, as well as to determine the Fermi surface dimensions and the properties of the carriers in the vicinity of the gap collapse. Resistance measurements were carried out in the portable dilution refrigerator on a carefully screened SmB_6 sample, which had been loaded in a Tozer-designed ultraminiature diamond anvil cell. An example of the sample magnetoresistance at 15 kbar, at the base temperature of 45 ± 5 mK is shown in Figure 2. This measurement suggests that the noise levels present in the portable dilution refrigerator are nearly low enough to continue the measurements into the fully metallic, gapless phase present above the critical pressure. Unfortunately, the pressure cell failed before we reached the critical pressure. We intend to repeat this experiment in the upcoming year.

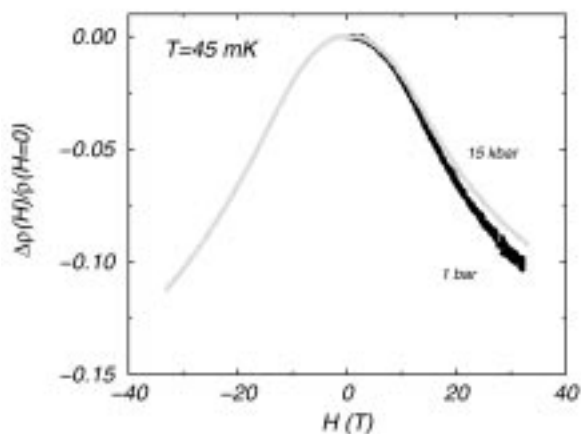


Figure 2. Magnetoresistance of SmB_6 at 45mK at 1 bar and 15 kbar.

Magnetic Field Dependence of the Thermal Excitations in $\text{YbNi}_2\text{B}_2\text{C}$ and $\text{LuNi}_2\text{B}_2\text{C}$

Beyermann, W.P., Univ. of California-Riverside, Physics

Lacerda, A.H., NHMFL/LANL

Canfield, P.C., Ames National Laboratory and Iowa State Univ., Physics

Schmiedeshoff, G.M., Occidental College, Physics

The specific heat was measured from 1.75 K to 20 K in the presence of an applied magnetic field on single-crystalline $\text{LuNi}_2\text{B}_2\text{C}$ and $\text{YbNi}_2\text{B}_2\text{C}$. These two compounds are members of the borocarbide series where an interesting interplay between superconductivity and magnetism exists. In the first system, a superconducting transition occurs at 16 K, with no evidence of magnetism at any other temperature. The second system is unique in the series because, in place of any kind of long-range order, a heavy Fermi-liquid ground state develops with a Kondo temperature of ~ 10 K.

Below the superconducting transition, the specific heat of $\text{LuNi}_2\text{B}_2\text{C}$, in zero field, is dominated by a T^3 temperature dependence where the thermal excitations are primarily due to lattice vibrations. By applying a magnetic field that exceeds the upper critical field, a measurement of the specific heat gives a good estimate of the phonon contribution, which can then be subtracted from the zero-field data. The remaining contribution has an exponential temperature dependence with a linear term from a small amount ($\sim 5\%$) of the sample that is normal, and fits of the subtracted data find a superconducting gap that is close to the BCS value.

When a magnetic field is applied to the sample, the linear temperature-dependent component in the specific heat increases. The Sommerfeld coefficient (C/T) determined from these data increases with increasing field, eventually

saturate at ~ 20 mJ/mol K² for fields equal to or above H_{c2} . This linear component to the specific heat is a consequence of three effects: (1) excitations from continuum states associated with the nodal structure, (2) core excitations from bound states localized in a vortex core, (3) vortex to vortex interactions. The measured field dependence of the Sommerfeld coefficient is very close to H^0 ,⁴¹ which was calculated¹ for an s-wave superconductor taking into account all three effects. Therefore both the temperature and field dependence of the specific heat below the superconducting transition are consistent with an s-wave superconducting ground state in LuNi₂B₂C.

For an enhanced Fermi-liquid ground state, one expects the Kondo peak in the specific heat at zero magnetic field to evolve into a Schottky-like anomaly characterizing an uncorrelated electron gas in a magnetic field as the applied field energy exceeds the Kondo interaction strength. A reduction in the Sommerfeld coefficient with increasing field is a consequence of this evolution.

In YbNi₂B₂C, a broad Kondo peak is observed in the specific heat. When measured in zero field, this peak is centered at ~ 10 K, and gradually moves to higher temperatures as the field is increased. The Sommerfeld coefficient also decreases. Often in theoretical treatments of this problem, a single energy scale determines both the thermodynamic and transport properties, making it possible to relate data from these different experiments. Qualitatively, the Sommerfeld coefficient and the T^2 coefficient for the electrical resistivity decrease with increasing applied magnetic fields; however deviations in the quantitative relationship between these quantities are observed.

Reference:

¹ Ichioka, M., *et al.*, preprint.

Magnetoresistance of the Non-Fermi-Liquid System UCu₄Pd

Beyermann, W.P., Univ. of California at Riverside, Physics

Lacerda, A.H., NHMFL/LANL

Chau, R., Univ. of California at San Diego, Physics

Maple, M.B., Univ. of California at San Diego, Physics

In preliminary measurements using a continuous field magnet, the transverse magnetoresistance of UCu₄Pd was found to be negative and small up to 18 T at all temperatures above 2 K. When the temperature was decreased, the magnitude of the effect increased without any sign of eventually turning positive, which is often observed in many systems with enhanced Fermi-liquid ground states at low temperatures.

With a short-pulsed magnet, these measurements were extended to 60 T. The normalized magnetoresistance data are displayed in Figure 1 as a function of field for two different temperatures. At both temperatures, the magnetoresistance remained negative to the highest fields and increased in magnitude when the temperature was lowered from 4 K to 2 K.

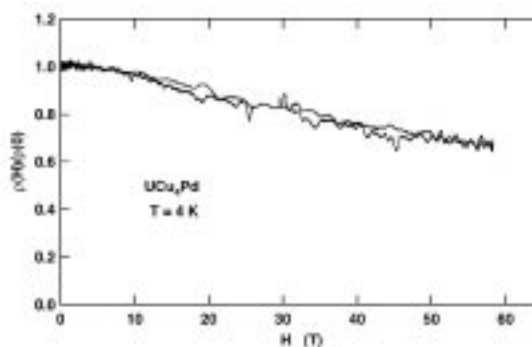


Figure 1. Magnetoresistance vs. magnetic field to 60 T.

Specific Heat Measurements on U_2Cu_9Al and $UCu_{3.5}Al_{1.5}$ in High Magnetic Fields

Beyermann, W.P., Univ. of California-Riverside, Physics
Torikachvili, M., San Diego State Univ., Physics
Lacerda, A.H., NHMFL/LANL
Nakotte, H., New Mexico State Univ., Physics

In recent investigations of the U-Cu-Al series, unusual electronic and magnetic properties have been observed at low temperatures. For example, two peaks are found at ~ 9.5 K and ~ 31 K in the specific heat of U_2Cu_9Al that were identified as some type of antiferromagnetic transitions. Below the lower transition, an enhanced contribution to the specific heat that is linear in temperature is present with a Sommerfeld coefficient of ~ 210 mJ/mol-U K². As the temperature is lowered from 300 K, the electrical resistivity at zero field decreases. Two small local maxima occur at 60 K and 27 K, after which there is an abrupt increase in the resistivity below 16 K. With the application of 18 T, the resistivity at 2 K drops $\sim 30\%$, resulting in a broad maximum at ~ 60 K, and a T² temperature region at low temperatures.

In order to investigate the thermodynamics of this dramatic field-induced change in the low-temperature resistance, the specific heat was measured between 1.75 K and 20 K in applied magnetic fields up to 18 T. The data, plotted as C/T versus T, are displayed in

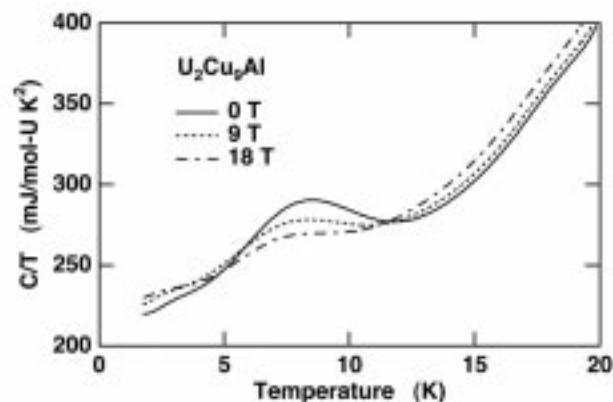


Figure 1. Heat capacity versus temperature.

Figure 1. In the presence of fields as high as 18 T, there is very little change in the specific heat, except for a small decrease in the amplitude of the peak associated with the magnetic transition at ~ 9.5 K, and a slight increase at higher temperatures, despite a significant shift in the transport to a metallic-like ground state.

Specific heat measurements were also performed on $UCu_{3.5}Al_{1.5}$. This system does not order magnetically, and the low-temperature specific heat and magnetic susceptibility show scaling behavior that is reminiscent of other non-Fermi liquid materials. The specific heat data collected in zero magnetic field are similar to that reported in the literature. Unfortunately, two attempts were made to apply a field, and in both cases the sample fell off the platform of the calorimeter during the field ramp, precluding the measurement.

References:

- 1 Prokes, N., *et al.*, to be published.
- 2 Nakotte, H., *et al.*, Phys. Rev. B, **54**, 12176 (1996).

SmB₆: Magnetoresistance to 60 Tesla

Cooley, J.C., LANL
Mielke, C.H., NHMFL/LANL
Harrison, N., NHMFL/LANL
Hults, W.L., LANL
Smith, J.L., LANL

The small gap insulators known as Kondo insulators are of interest because they are compounds with all the ingredients needed to be heavy fermion metals, but are instead insulators. Recent flux compression experiments¹ on single crystals of the Kondo insulator SmB₆ suggested that the insulating gap, determined from the resistivity, may close near 85 T. The data below 30 T in the flux compression experiment, however, is lost due to ringing in the transmission line. The goal in this work was to measure the magnetoresistance of SmB₆ crystals from the same batch, up to 60 T, to

see if it agreed with the flux compression experiment.

A four-probe dc resistivity measurement was chosen because the flux compression experiment was a dc resistance measurement. Field pulses were made for each current polarity, allowing us to easily remove pickup induced voltages. Shown in Figure 1 is the magnetoresistance up to 60 T at 4 K taken in the 60 T pulsed magnet and the magnetoresistance up to 145 T from the flux compression experiment, both normalized to the zero field value. The agreement of the two data sets is quite good, which suggests that the flux compression data is reliable. As part of our ongoing investigation of this system, we have measured the magnetization at 4 K to 60 T. The magnetization is nearly linear to 60 T with no indication of saturation.

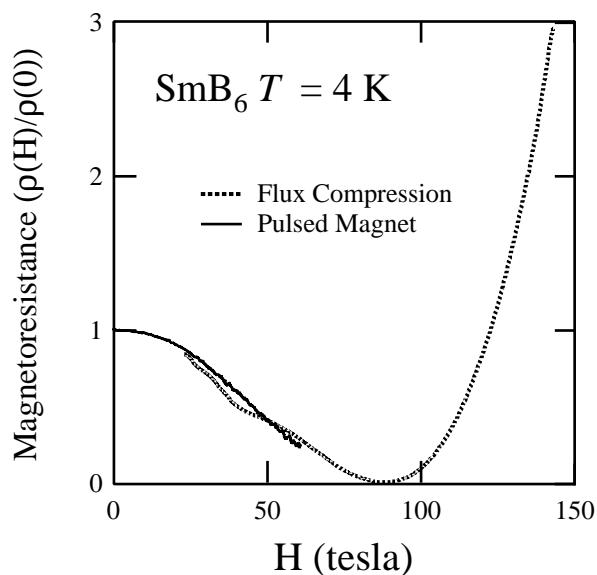


Figure 1. The magnetoresistance of SmB_6 at 4 K from both pulsed magnet and flux compression experiments.

Reference:

- 1 Cooley, J.C., *et al.*, J. Superconductivity, accepted for publication.

De Haas-van Alphen Measurements on USn_3 and UAl_3

Cornelius, A.L., LANL

Arko, A.J., LANL

Sarrao, J.L., LANL

Hundley, M.F., LANL

Thompson, J.D., LANL

Booth, C.H., LANL

Harrison, N., NHMFL/LANL

Oppeneer, P.M., Inst. of Theoretical Physics, Univ. of Technology, Dresden, Germany,

The uranium compounds UX_3 , where X is a IIIA or IVA element, crystallize in the cubic AuCu_3 -type structure. Due to the cubic crystal structure, the wide range of hybridization strengths, and the availability of high-quality single crystals, UX_3 compounds are excellent for examining how the measured physical properties and underlying electronic structure are interrelated.

We have performed de Haas-van Alphen (dHvA) measurements in pulsed fields to 50 T on the compounds USn_3 and UAl_3 and have previously reported results on UGa_3 . The measurements were performed along the (100) axis of the cubic crystal. The electronic specific heat coefficient of 173 mJ/mol K^2 for USn_3 makes this a heavy-fermion system, while UAl_3 is believed to be a spin fluctuator. When the magnetic signal is plotted versus the inverse field, one observes oscillations with a frequency that is directly proportional to an extremal area of the Fermi surface; this is the dHvA effect. In Figure 1, there are plots of the fast Fourier transform (FFT) of the signal versus inverse field USn_3 in (a) and UAl_3 in (b). Though numerous peaks appear in the FFT for USn_3 , all but the peak labeled with an asterisk (*), at a frequency of $F = 2080$ T, can be attributed to Sn impurities. From the temperature dependence of the FFT amplitude, we estimate that $5 < m^*/m_e < 15$ for this frequency. UAl_3 also only shows a single peak at $F = 2510$ T. The effective mass of the observed frequency is

$1 < m^*/m_e < 4$. These results, along with our previous measurements on UGa_3 can well be explained by band structure calculations that show that the electronic structure and physical properties can be related to the degree of 5f-electron delocalization.

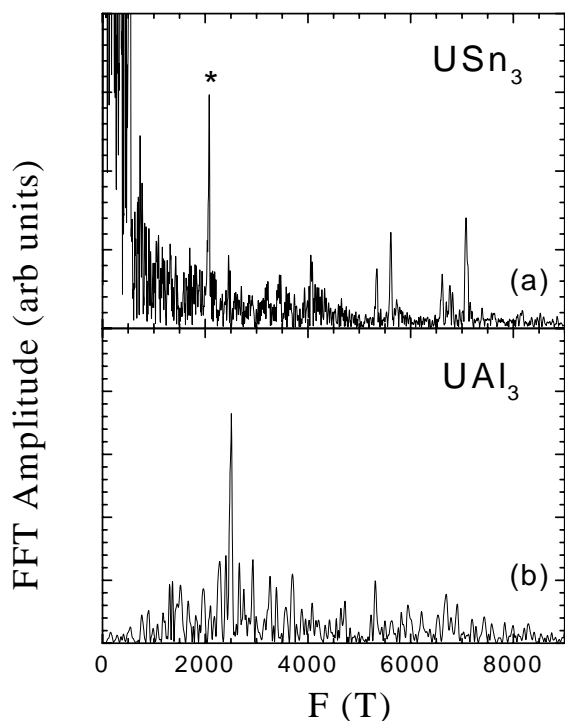


Figure 1. The fast Fourier transforms (FFT) of the de Haas-van Alphen signal measured at $T=0.5$ K for USn_3 in (a) and UAl_3 in (b). Only the peak labeled with an asterisk (*) in (a) is due to USn_3 .

Magnetization and de Haas-van Alphen Measurements to 50 T on U_2Zn_{17}

Cornelius, A.L., LANL
 Arko, A.J., LANL
 Sarrao, J.L., LANL
 Smith, J.L., LANL
 Harrison, N., NHMFL/LANL
 Fisk, Z., NHMFL/FSU

U_2Zn_{17} is a well-studied, heavy-fermion compound. It crystallizes in the Th_2Zn_{17} hexagonal structure and orders antiferromagnetically at 10 K. The structure is rather anisotropic with antiferromagnetically

coupled nearest neighbors, with U-U spacings of 4.36 Å along the hexagonal axis and 5.16 Å in the basal plane. Previous work on single crystals has shown that there is not a large amount of anisotropy in the low temperature magnetic susceptibility. We have extended these measurements to lower temperatures and higher fields by measuring the magnetization and de Haas-van Alphen (dHvA) effect in pulsed fields to 50 T. The measurements were performed on a cylindrical sample with the cylindrical axis along hexagonal c-axis. The magnetization measurements are shown both perpendicular $B \perp c$ to (a), and along $B \parallel c$ (b) the cylindrical axis in Figure 1. The measurements were normalized using the results of previous low field measurements. For $B \perp c$, no magnetic transitions are observed and the magnetization increases slightly as the temperature is increased. For $B \parallel c$, there is a magnetic transition at $B=33$ T for $T=0.5$ K, which moves to smaller fields as temperature is increased, and is not observed at $T=9$ K. The magnetization decreases as temperature is increased in contrast to $B \perp c$. When the signal is plotted versus the inverse

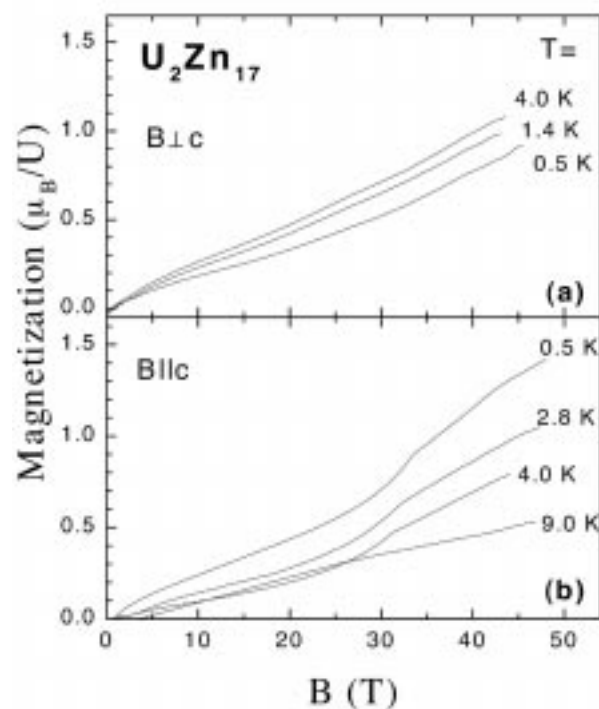


Figure 1. The measured signal magnetization versus applied pulsed magnetic field for U_2Zn_{17} for $B \perp c$ (a) and $B \parallel c$ (b), for various temperatures.

field, one observes oscillations in the signal with a frequency that is directly proportional to an extremal area of the Fermi surface; this is the dHvA effect. We observe a single dHvA frequency for $B||c$ above the magnetic transition with a frequency of 450 T and an effective mass of $\sim 4 m_e$.

Magnetization of UBe_{13} to 60 T

Detwiler, J.A., Occidental College, Physics
Schmiedeshoff, G.M., Occidental College, Physics
Harrison, N., NHMFL/LANL
Lacerda, A.H., NHMFL/LANL
Mielke, C.H., NHMFL/LANL
Smith, J.L., LANL

One of the more remarkable aspects of the heavy fermion superconductor, UBe_{13} , is the linearity of its isothermal magnetization in high magnetic fields. Early characterizations of the magnetization specify deviations from linearity in terms of a few percent at some large field. We have measured the magnetization of UBe_{13} in pulse fields to 60 T and at temperatures from 4.0 K to 0.5 K, in an effort to extract more quantitative information on the shape of $M(H)$, and to search for possible metamagnetic transitions, such as have been observed in other heavy fermion superconductors, UPt_3 for example.¹

We studied a needle-like single crystal of UBe_{13} (with its long axis parallel to the field) to minimize eddy current heating, and calibrated the magnetization signal assuming a low temperature susceptibility of 15 memu/mol-G. The data exhibited a very small temperature dependence consistent with low field susceptibility data in the literature.²

We observed an approximate 20% depression of $M(H)$ below linearity near 60 T at 0.5 K. The shape of $M(H)$ is well fit by a Brillouin function with $j=1/2$, and a saturation moment of about $2 \mu_B/U$ -atom. The saturation moment is in reasonably good agreement with the high temperature moment of about $3.4 \mu_B/U$ -atom, derived from low field

susceptibility measurements in the literature.² This agreement does not support the hypothesis of a metamagnetic transition at higher fields.

References:

- 1 Franse, J.J.M., *et al.*, *Physica B*, **163**, 511 (1990).
- 2 Stewart, G.R., *Rev. Mod. Phys.*, **56**, 755 (1984) and references therein.

High Field Magnetoresistance of the Non-Fermi-Liquid Alloys $U_{1-x}Th_xPd_2Al_3$ and $U_{1-x}Y_xPd_2Al_3$

Dickey, R.P., Univ. of California, San Diego (UCSD), Physics, and Institute for Pure and Applied Physical Sciences
de Andrade, M.C., UCSD, Institute for Pure and Applied Physical Sciences
Freeman, E.J., UCSD, Physics, and Institute for Pure and Applied Physical Sciences
Maple, M.B., UCSD, Physics, and Institute for Pure and Applied Physical Sciences

We have performed magnetoresistance measurements at the NHMFL-LANL, using a 3He - 4He dilution refrigerator in the temperature range $20 \text{ mK} \leq T \leq 2.5 \text{ K}$ and a 20 T superconducting magnet. Measurements were made on two different kinds of uranium-based materials that exhibit non-Fermi-liquid behavior in their physical properties at low temperatures, $U_{1-x}Th_xPd_2Al_3$ and $U_{1-x}Y_xPd_2Al_3$. Previous measurements of R vs. T on the $U_{1-x}Th_xPd_2Al_3$ system, for $x = 0.2, 0.4, 0.6, 0.9$ and 1.0 , display a small, negative magnetoresistance for fields up to 18 T. The sample with thorium concentration, $x = 0.6$, also exhibits an unusual temperature dependence with increasing field. For small fields below roughly 8 T, the resistivity saturates at low temperatures with a negative slope as $T^{3/2}$. For fields near 8 T, the resistivity saturates at low temperatures as a nearly temperature independent constant, and for larger fields up to 18 T, the resistivity saturates with a positive slope. In new measurements of a sample with thorium concentration, $x = 0.8$, we

find similar behavior, including the change from negative slope at low fields to positive slope at high fields. The origin of this behavior is unknown at this time, but is believed to be related to the competition between the RKKY interaction, which results in antiferromagnetic order for small thorium concentrations, and the Kondo effect, which is known to be present at high thorium concentrations.

Previous measurements of R vs. T , on a $U_{0.2}Y_{0.8}Pd_2Al_3$ sample, exhibited a resistivity that has a linear temperature dependence at low temperatures and a small negative magnetoresistance. New measurements for the $U_{1-x}Y_xPd_2Al_3$ system with $x = 0.2, 0.4, 0.6, 0.7,$ and 0.9 are consistent with this result. For the samples with concentrations less than $x = 0.7$, the resistivity saturates at low temperatures approximately as T^2 . For the sample with $x = 0.7$, the linear temperature dependence of the resistivity is very similar to what was previously seen for $x = 0.8$. At temperatures below approximately 300 mK, however, the resistivity appears to saturate to a constant, which was not the case for the $x = 0.8$ sample. The sample with yttrium concentration, $x = 0.9$, has an upturn at low temperatures which is likely due to Kondo scattering.

Correlated Electron Materials

Fisk, Z., NHMFL/FSU, Physics
Immer, C., NHMFL/FSU, Physics
Jackson, D., NHMFL/FSU, Physics
Torelli, M., NHMFL/FSU, Physics
Young, D., NHMFL/FSU, Physics

Our research has focussed in three different classes of materials: $YbRCu_4 C15_b$ materials, hexaborides, and layered perovskite oxides. We describe our progress for each of these below.

(1) The first-order isostructural valence transition in $YbInCu_4$ has been studied as a function of applied pressure, and external magnetic field, both in the pure material and in materials doped on the Yb, In and

Cu sites. All the data for the magnetic field dependence of the structural phase transition fall onto a single phase diagram in reduced magnetic field and temperature variables. These data indicate that there is a single energy scale for the valence transition, which suggests that the first-order phase transition may be fundamentally a second-order phase transition. A comparative study has been made as well on the isostructural $YbInNi_4$. Additionally, a series of single crystal materials have been studied, in which, In has been replaced. Among these, $YbTiCu_4$ appears to be an intermediate valence material, with properties reminiscent of $CePd_3$. The conclusion from these studies, and earlier studies, is that the Kondo volume collapse model does not describe well the phase transition in $YbInCu_4$, and that the transition appears to be closely related to the low electronic density of states present in the high temperature phase.

(2) We have continued our collaborative studies on rare earth and alkaline earth hexaborides. In the ferromagnet EuB_6 , a Raman investigation done on our crystals by S. L. Cooper found certain strong similarities between the physics of the manganites and EuB_6 . De Haas-van Alphen work in collaboration with R. G. Goodrich found oscillation consistent with electron and hole ellipsoids near the X-point in the Brillouin zone as predicted by band theory. Fermi surface in collaboration with Goodrich, D. Hall and N. Harrison on LaB_6 has discovered quantum interference orbits, only the second three-dimensional metal, in which, these Stark orbits have been observed. These orbits were subsequently observed in CeB_6 as well. In addition, the Fermi surface of the alloy series $La_{1-x}Ce_xB_6$ has been measured across the entire range of x , the first such system for which this has ever been accomplished, and particularly surprising in view of the fact that Ce is a Kondo ion in this compound. Another quite unexpected discovery has been high temperature ferromagnetism in electron doped CaB_6 . For 0.005 La doping, the ordered moment is $0.07\mu_B/La$ and the ordering temperature $T_c=600K$. For $x=0.01$, the ordered moment is approximately an order of magnitude less, with $T_c=950K$, essentially that of pure Fe.

(3) We have collaborated with Hammel on a study of antiferromagnetic order in lightly doped

$\text{La}_2\text{Cu}_{1-x}\text{Li}_x\text{O}_4$ using La-139 NQR. The important result of this study is that the apparently stationary holes introduced by the Li-doping behave with respect to the antiferromagnetic order and internal field exactly like the mobile holes that can be introduced by Sr-doping of La_2CuO_4 . A satisfactory explanation for this has not been found.

The dHvA Effect in $\text{La}_{1-x}\text{Ce}_x\text{B}_6$

Goodrich, R.G., Louisiana State Univ., Physics
Harrison, N., NHMFL/LANL
Young, D., NHMFL
Fisk, Z., NHMFL

In this work we measured the dHvA effect on random alloys of $\text{La}_{1-x}\text{Ce}_x\text{B}_6$ in which samples with values of x between 0 and 1 in sixteen steps were measured. Unlike other alloy systems involving magnetic impurities, strong signals are observed across the entire series. We see that as x is changed the Fermi surface (FS) of CeB_6 smoothly evolves from the FS of LaB_6 . This evolution begins at very low concentrations and includes changes in the topology, effective masses and spin polarization of the FS.

Single crystal samples of $\text{La}_{1-x}\text{Ce}_x\text{B}_6$ with compositions of $x = 0$ to 1 in 0.1 and 0.05 steps were grown in Al flux. Signals from the oscillatory magnetic susceptibility occurring due to the dHvA effect were measured with the field applied along the $\langle 100 \rangle$ axis in pulsed magnetic fields up to 60 T at the NHMFL, Los Alamos. The sample temperature could be controlled between 0.4 and 4 K by immersing the sample-pickup coil arrangement in ^3He and ^4He reservoirs.

The fact that dHvA oscillations are observed at intermediate values of x immediately indicates that a coherent Fermi liquid exists with surprisingly long quasiparticle lifetimes. Strong signals are observed at all concentrations of Ce and the measured frequencies lie between those of pure LaB_6 and pure CeB_6 . The FS of trivalent (RE) B_6 compounds (where RE = rare earth) is a result of energy bands

that arise from the transfer of electrons from the RE to the boron octahedra. The Fermi energy is such that six prolate electron ellipsoids situated at the X points of the Brillouin zone (BZ) exist and slightly overlap along the ΓR symmetry axes of the BZ. With the magnetic field directed along a $\langle 100 \rangle$ crystal axis, a frequency corresponding to the minimum cross sectional area of this ellipse can be directly observed, and a frequency from the maximum area is observed through magnetic breakdown (MB) occurring at the overlap points. Both of these frequencies are observed along with several harmonics at all concentrations.

A large number of measurements now have been performed on LaB_6 ,¹ a good metal, and on CeB_6 ,² which is regarded as a typical dense Kondo lattice with a very low Kondo temperature of 1 K to 2 K. Studies of CeB_6 have enabled rather extensive comparisons between experiment and theory to be made, because CeB_6 is one of the only HF materials in which one can observe almost the entire Fermi surface topology through dHvA measurements.³ The present results show that this fact is also preserved on alloying, and that a coherent Fermi liquid ground state indeed exists for all compositions of $\text{La}_{1-x}\text{Ce}_x\text{B}_6$, in spite of the disorder. This data allows us to observe for the first time, the topological changes of the Fermi surface to be seen as the concentration of Ce is increased, and as the heavy Fermion ground state develops. As the frequencies change the ellipsoid volume and number of carriers changes. Also the effective mass change starts out linear, becomes quadratic in x , and then experiences a maximum near $x = 0.9$. Over the $x = 0.2$ to 0.8 quadric range the result is consistent with the model given by Gor'kov and Kim.⁴ Finally, the FS appears to be spin polarized for all concentrations greater than 0.05 Ce.

References:

- 1 Arko, A.J., *et al.*, Phys. Rev. B, **13**, 5240 (1976).
- 2 Harrison, N., *et al.*, Phys. Rev. Lett., **81**, 870 (1998).
- 3 Chapman, S., *et al.*, J. Phys.: Condens. Matter, **2**, 8123 (1990).
- 4 Gor'kov, L.P., *et al.*, Phys. Rev. B, **51**, 3970 (1995).

Effect of Pressure and Magnetic Field on the Heavy Fermion Superconductor $U(\text{Pt},\text{Pd})_3$

Graf, M.J., Boston College, Physics

de Visser, A., Univ. of Amsterdam, Van der Waals - Zeeman Inst.

Keizer, R.J., Univ. of Amsterdam, Van der Waals - Zeeman Inst.

Hannahs, S.T., NHMFL

We are investigating the phase diagram of $U(\text{Pt}_{1-x}\text{Pd}_x)_3$ near the point $x = 0.007$, $T = 0$ K, where superconducting and static antiferromagnetic phase lines meet.¹ Polycrystalline $U(\text{Pt}_{0.996}\text{Pd}_{0.004})_3$ was studied to search for quantum critical behavior as $T_c \rightarrow 0$ K.² The rate of suppression of T_c with pressure is nearly twice that for pure UPt_3 , while the normal-state resistivity shows that rate of increase of the spin-fluctuation temperature T_{SF} with pressure is increased over that for pure UPt_3 . Thus the close connection between spin-fluctuations and superconductivity is maintained with addition of Pd. The low-field (< 7 T) magnetoresistance is unaffected by pressure; at higher fields we find a reduction in the magnetoresistance with increasing pressure, caused in part by the suppression of the high-field pseudo-metamagnetic transition. No qualitative changes occur in the transport as $T_c \rightarrow 0$ K, and UPt_3 appears not to have a superconducting quantum critical point. We are now focusing on the

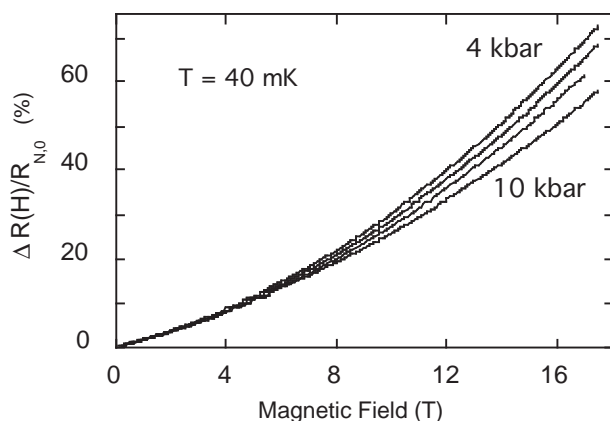


Figure 1. Magnetoresistance for pressures of 4, 5.5, 7.5, and 10 kbar.

observation of quantum critical behavior associated with the onset of static antiferromagnetism. This work is supported through Research Corporation award RA0246.

References:

- 1 Graf, M.J., *et al.*, *Physica B* (in press).
- 2 Ramazashvili, R., *et al.*, *Phys. Rev. Lett.*, **79**, 3752 (1997); Ramazashvili, R., *Phys. Rev. B*, **56**, 5518 (1997).

CeB_6 in Strong Magnetic Fields

Harrison, N., NHMFL/LANL

Hall, D.W., NHMFL

Goodrich, R.G., Louisiana State Univ., Physics

Vuillemin, J.J., Univ. of Arizona, Physics

Fisk, Z., NHMFL

There has been a renewed interest recently in the behavior of heavy fermion systems in strong magnetic fields. CeB_6 , while being relatively light compared to some of the super-heavy heavy fermion compounds, is somewhat unique in that pretty much all of its Fermi surface appears to be observable;¹ at least for one spin sheet. It also has an unusual antiferromagnetic ground state, but reverts to what is believed to be an antiferroquadrupolar phase at fields above ~ 2 T, accompanied by a saturation of the magnetization at approximately $1 \mu_B$ per formula unit.² The sudden jump in the magnetization at ~ 2 T is indistinguishable from the theoretical form expected for a metamagnetic transition, according to Edwards and Green for a spin $1/2$ system.^{3,4} Because of its cubic crystallinity, however, the ground state of the $4f$ moments is actually expected to be a Γ^8 quartet. Therefore, like most other heavy fermion systems, this material is clearly not well understood.

Above the transition, where the de Haas-van Alphen oscillations are observed, it has been well established for many years that the quasi-particle effective masses fall dramatically with increasing field.⁵ Some of our more recent experiments in

fields of up to 60 T (using the short pulse magnets) have revealed a number of new and surprising effects.⁶ Like its non- f -electron La analogue,⁷ CeB₆ shows quantum interference effects; one of the frequencies corresponding to an area in k -space equal to the Brillouin zone with an effective mass of zero. This, and other quantum interference frequencies, enables the topology of the Fermi surface to be determined in a straight forward manner at high magnetic fields, and reveals that the Fermi surface is actually changing in shape as a function of the applied field. A cartoon of the change in the Fermi surface is shown in Figure 1. This behaviour cannot be accounted for by the theory for the de Haas-van Alphen effect in heavy fermion systems by Wasserman *et al.*,⁸ and suggests that a rigid band-like approach is not appropriate. Indeed, it is no surprise that the mean field theory of Wasserman, *et al.*, breaks down, since the field at which the de Haas-van Alphen oscillations are observed is roughly 30 times higher than the metamagnetic transition (where $B = T_{\text{Kondo}}$), and therefore 30 times higher than the anticipated limit of the mean field approach.^{6,8}

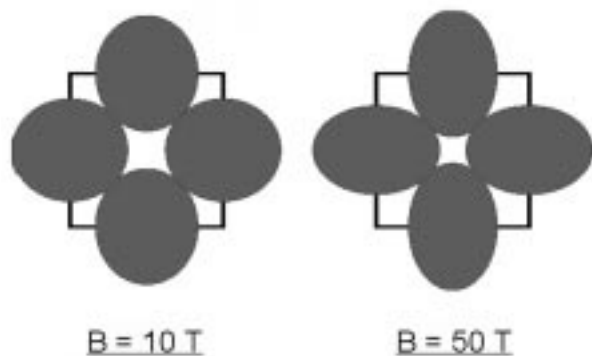


Figure 1. A schematic representation of the change in the topology of the Fermi surface of CeB₆ on increasing the magnetic field from 10 T to 50 T. The illustration is for a cross-section through the GXM-plane of the Brillouin zone.

Another intriguing observation is that the de Haas-van Alphen oscillations originate from a Fermi surface of only one spin.⁶ This does not mean that there is only one spin, but rather that one of the spin components is unobservable for some reason. One of the possible reasons is that it just has a heavier mass. Both the model of Wasserman, *et al.*,⁸ and that of Edwards and Green,³ expect one

of the spins to have a heavier mass, although the models do not agree on which spin this should be, nor on the mechanism by which the heavy mass comes about at high magnetic fields. The model of Edwards and Green does have the advantage of being more applicable at high magnetic fields above the metamagnetic transition where the system is thought to be behaviorally similar to an itinerant ferromagnet.³ In this case, we should expect the spin down electrons to be strongly enhanced by spin fluctuation effects. Specific heat measurements, however, indicate that the unobservable spin sheet is not heavy enough to prevent us from being able to see it, given the apparent sensitivity of the de Haas-van Alphen experimental technique.⁶

Future work clearly needs to address the question of the origin of the spin polarization, as well as the applicability of the Anderson lattice model in this and other heavy fermion compounds. There are alternative descriptions which could apply; i.e. according to Aoki *et al.*, the Anderson lattice model may not apply, and instead they claim that their results support a picture in which band structure calculations are able to reproduce the experimental observations either with or without f -electrons included (depending on whether the magnetic field is above or below the metamagnetic transition).⁹ An all-encompassing theory, which unifies band structure-type properties of the f -electrons with the many-bodied Anderson lattice-like properties of the f -electrons, still needs to be developed.

Some of the work mentioned here contributed to Donovan Hall's thesis at Louisiana State University.

References:

- 1 Onuki, Y., *et al.*, J. Phys. Soc. Japan, **58**, 3698 (1989).
- 2 Komatsubara, T., *et al.*, J. Magn. Mater., **31 & 34**, 368 (1983).
- 3 Edwards, D.M., *et al.*, Z. Phys. B, **103**, 243 (1997).
- 4 Edwards, D.M., Physica B, **169**, 271 (1991).
- 5 Joss, W., *et al.*, Phys. Rev. Lett., **59**, 1609 (1987).
- 6 Harrison, N., *et al.*, Phys. Rev. Lett., **81**, 870 (1998).
- 7 Harrison, N., *et al.*, Phys. Rev. Lett., **80**, 4498 (1998).
- 8 Wasserman, A., *et al.*, J. Phys.: Condens. Matt., **1**, 2669 (1989).
- 9 Aoki, H., *et al.*, Phys. Rev. Lett., **71**, 2110 (1993).

Fermi Surface Studies of XBe_{13} Compounds

Harrison, N., NHMFL/LANL

Cornelius, A.L., LANL

Smith, J.L., LANL

Schmiedeshoff, G.M., Occidental College-California,
Physics

Detwiler, J.A., Occidental College-California, Physics

Harima, H., Osaka Univ., Physics

Takegahara, K., Hirosaki Univ., Physics

There exist a large number of XBe_{13} compounds, with X referring to a rare earth or actinide element. However, no definitive Fermi surface measurements have been reported for any of these. Perhaps UBe_{13} is the most exotic of these compounds, although $NpBe_{13}$, $CeBe_{13}$, and $PuBe_{13}$ all show signs of strongly correlated behavior. An understanding of the electronic structure is of considerable importance if we are to understand these systems in detail.

Ultimately, we would like to learn more about the electronic structure of UBe_{13} , which has so far been reluctant to yield quantum oscillations. This can be for either of three reasons; one, the ground is a non-Fermi liquid; two, the effective masses are exceptionally high; or three, the crystals are just too dirty. We can already eliminate the third possibility, since we have succeeded in observing

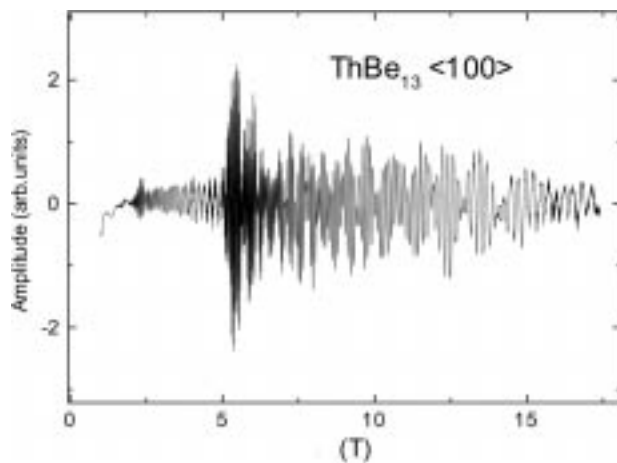


Figure 1. An example of de Haas-van Alphen measurements made on $ThBe_{13}$.

de Haas-van Alphen oscillations in $ThBe_{13}$, which is very similar from the chemical point of view. Figure 1 shows an example of de Haas-van Alphen measurements made in $ThBe_{13}$. Preliminary studies appear to show that the measurements are largely consistent with the calculated band structure. It should be noted that the quantum oscillations are observed down to very low fields, which is clearly indicative of a high quality sample. Quantum oscillations have also been observed in powdered samples of $PrBe_{13}$.

An alternative way of investigating the development of the heavy fermionic ground state in UBe_{13} , is to study $ThBe_{13}$ and then observe the changes in the electronic structure as Th is substituted with U . Preliminary investigations show that things have already changed radically as soon as 5% U is added.

Magnetic Impurities in Unconventional Fermi Systems

Ingersent, K., UF, Physics/NHMFL

Gonzalez-Buxton, C., UF, Physics

Si, Q., Rice Univ., Physics

Certain anisotropic superconductors, zero-gap semiconductors, and phases of the two-dimensional electron gas in a magnetic field exhibit a quasiparticle density of states that vanishes in a power-law fashion at the Fermi energy. There is now strong evidence that the cuprate high- T_c superconductors belong to this class of materials, and several heavy-fermion superconductors are also strong candidates.

Magnetic impurities in such systems are expected to exhibit a range of remarkable behaviors that have no counterpart in metallic hosts. In particular, the single-impurity Kondo model in which the conduction-band density of states has a power-law pseudogap at the Fermi energy is known to exhibit a zero-temperature phase transition at a finite exchange coupling. Prior work has focused on the low-temperature physics of the weak- and strong-coupling regimes.¹ We have recently elucidated²

the critical properties of the transition itself, both for $N = 2$ and for $N \gg 1$, where N is the spin degeneracy. The critical exponents are consistent with a simple scaling form for the free energy. For any finite N , the temperature exponent of the local spin susceptibility at the critical Kondo coupling varies continuously with the power of the pseudogap. This observation has motivated us to investigate whether a single-particle pseudogap produces an anomalous local spin response in certain heavy-fermion metals close to a magnetic quantum critical point, an anomaly evidenced³ by neutron scattering experiments on $\text{CeCu}_{6-x}\text{Au}_x$.

References:

- 1 See Gonzalez-Buxton, C., *et al.*, Phys. Rev. B, **57**, 14254 (1998), and references therein.
- 2 Ingersent, K., *et al.*, preprint (cond-mat/9810226).
- 3 Schröder, A., *et al.*, Phys. Rev. Lett., **80**, 5623 (1998).

Heat Capacity Experiments in the New Long Pulse 60 T Magnet



Jaime, M., LANL
 Movshovich, R., LANL
 Stewart, G.R., Univ. of Florida, Physics
 Beyermann, W.P., Univ. of California-Riverside,
 Physics

We have built a plastic probe that allows heat capacity measurements at temperatures between 1.6 K and 20 K, in pulsed fields. The Si platform, suspended from a G-10 frame with Nylon strings, is equipped with heater and thermometer, and is weakly thermally connected to a temperature regulated block (TRB). To maximize the available experimental space, a novel vacuum tapered seal, made out of G-10 and 1266 Stycast epoxy, was developed. The differential thermal contraction between the parts aids in producing a superfluid-tight joint. The thermal equilibrium time constants for the TRB and the Si platform are on the order of minutes, see Figure 1. During the magnetic field pulse, which is 2 seconds long, both the TRB and

the heat capacity platform are thus under an adiabatic condition. The sample's internal thermal relaxation time constant, τ_{int} , $\sim 10^{-3}$ s at a temperature of a few Kelvin, grows rapidly as the temperature increases. At low temperatures, the time constant of the heat capacity stage (τ_{st}) can again increase due to either electronic and/or nuclear magnetic entropy of the sample or decrease due to the boundary thermal conductivity. The temperature interval between 1 K and 20 K is, therefore, a convenient starting point for developing heat capacity measurements in pulsed magnetic fields.

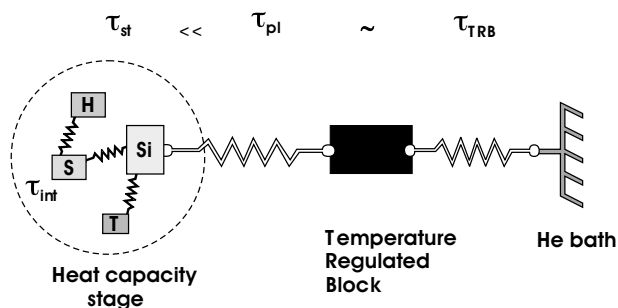


Figure 1. Schematic diagram of the pulsed field calorimeter, showing thermal links and thermal relaxation times (τ) between the different components. Both the heat capacity stage and the TRB are in vacuum during the experiment.

We use a heat pulse method to measure heat capacity, where a known amount of heat is delivered to the sample using a chip resistor. The heat capacity stage must come to equilibrium both before and after the heat pulse is delivered while the magnetic field remains constant. The flat field plateau of the Long Pulse (LP) 60 T magnet allows this to occur. The temperature of the stage is measured with a Cernox chip resistant thermometer, calibrated in both dc fields up to 30 T, and pulsed fields up to 60 T. The heat capacity of the sample is then determined as the ratio of the heat delivered to the sample to the change in its temperature.

As an example of a heat capacity experiment, Figure 2 shows a 60 T pulse, the temperature evolution of the empty Si platform, and several heat pulses delivered to the platform. The thermometer indicates a small temperature increase (0.5 K from

the ~ 4 K base temperature) as the magnetic field increases, due to the magnetocaloric effect. The short thermal relaxation time (τ_{st}) of the stage allows it to reach equilibrium within the 5 ms long heat pulse.

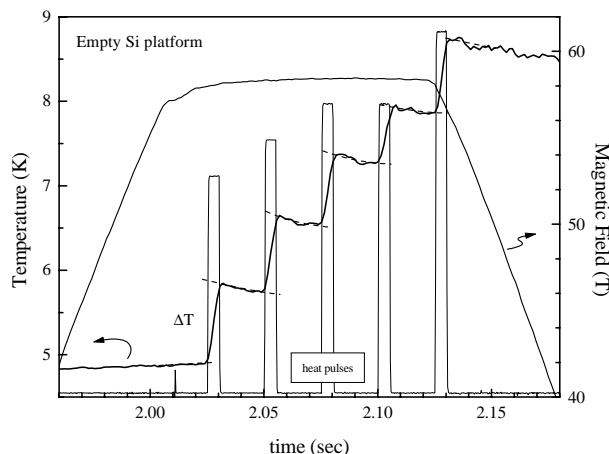


Figure 2. Magnetic field vs. time during a typical 60 T shot in the LP 60 T magnet, right axis. Temperature trace during the experiment, result of a train of heat pulses delivered to the stage with a $1\text{K}\Omega$ chip resistor, left axis. Voltage pulses in the heater are 5 ms long, the displayed scale correspond to a fraction of a volt.

We have demonstrated the feasibility of heat capacity measurements in the pulsed magnetic fields provided by the LP 60 T magnet at NHMFL/LANL. Direct measurement of heat capacity at field plateaus was clearly demonstrated. It appears that thermal equilibrium can be achieved even during the field sweep, given the low ramp rates the LP 60 T magnet is capable of achieving. In this situation, thermodynamic data can be obtained via the magnetocaloric effect from the temperature vs. field traces and magnetization data. Other types of thermal relaxation-related experiments, like thermal conductivity and Seebeck effect, are also under development.

This work was conducted under the auspices of the Department of Energy, and supported by the In-House Research Program of the NHMFL. We thank J. Kim for the calibration of our thermometer in 30 T, dc fields at the NHMFL-Tallahassee.

Heat Capacity of YbInCu_4 at Very High Magnetic Fields

NHMFL

Jaime, M., LANL
Movshovich, R., LANL
Sarrazo, J.L., LANL

The magnetic field produced with the Long Pulse 60 Tesla (LP 60 T) magnet is characterized by the low ramp rate of $\text{dB}/\text{dt} \leq 400$ T/s, and constant field plateaus of as long as 0.1 s at 60 T. We have built a probe made mostly of plastic materials, which allows us to perform measurements in a vacuum down to a temperature of 1.6 K, in fields up to 60 T. We use a heat pulse method to measure heat capacity, where a known amount of heat is delivered to the sample using a chip resistor as a heater element. The heat capacity of the sample is determined as the ratio of the heat delivered to the sample to the change in its temperature.

Metallic YbInCu_4 undergoes a first order valence phase transition at 42 K in zero field, where the specific volume is increased by 0.5% upon cooling,¹ with accompanying rise in the Kondo temperature (T_K) from 25 K to 500 K.² It is believed that, unlike in the case of Ce, where the phase transition is described within a Kondo-collapse scenario, the valence transition in YbInCu_4 is driven by the band structure effects.³ The complete magnetic field temperature phase diagram was obtained in dc Bitter magnets at NHMFL-Tallahassee and in capacitor-driven pulsed magnets at NHMFL-Los Alamos.⁴ This work showed that the transition can be suppressed down to $T = 0$ K with an applied field of 34.3 T.

The length of the flat top can be close to 0.5 s in the LP 60 T magnet for magnetic fields less than or equal to 40 T. A sequence of heat pulses can be delivered to the sample within the flat portion of the field profile, with sufficient time for our calorimeter to come to equilibrium before and after

each of the heat pulses. This situation is illustrated in Figure 1a for a field of 20 T, where a sequence of five, 10 ms long, heat pulses are delivered to the heat capacity stage during the plateau. The thermometer comes to equilibrium after the heat pulse is delivered well before the next heat pulse, and temperature is determined before and after each of the pulses. In this way a series of five $C_H(T)$ data points are collected in a single "shot" experiment, as the initial temperature for each of the heat capacity experiments is increased due to the previous heat pulse. The data from this, and one zero field "shot," is shown in Figure 1b. We fit the data with a sum of electronic and phononic terms ($A_H T + B_H T^3$). For zero field we obtained $A_0 = 49.5 \pm 0.4$ mJ/molK² and $B_0 = 0.85 \pm 0.03$ mJ/molK⁴. The value of A was in excellent agreement with available data in the literature.³ At 20 T we obtained $A_{20} = 80 \pm 5$ mJ/molK² and $B_{20} = 0.81 \pm 0.07$ mJ/molK⁴. The magnitude of the cubic term due to phonons was field-independent as expected. The increase of the linear term with field was likely due to scaling with magnetic field observed for various properties of YbInCu₄.

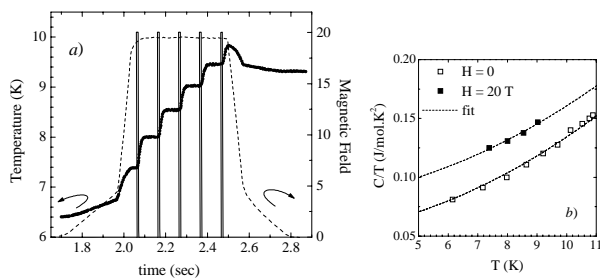


Figure 1. Multiple heat capacity experiments on YbInCu₄ during a single 20 T, 0.5 long pulse. *a)* Dashed line – magnetic field. Solid line – voltage applied to the resistive heater. • - Thermometer's trace. *b)* □ - specific heat at H = 0 collected with our probe. ■ - specific heat at H = 20 T obtained from data in *a)*.

A series of plateaus at different magnetic fields can be produced in the LP 60 T within a single experiment. Figure 2 displays the data for one such experiment, with four plateaus at 25, 30, 35, and 40 T, each 130 ms long. At each of the magnetic field plateaus the heat pulse is applied to the stage, and a heat capacity experiment is performed. In addition, as the field was changed between 30 T

and 35 T through the first order phase boundary, the temperature of the sample was observed to go down on the up-sweep, and up on the down-sweep, due to the magnetocaloric effect. These features are very sharp, and allow direct determination of the phase diagram of YbInCu₄.

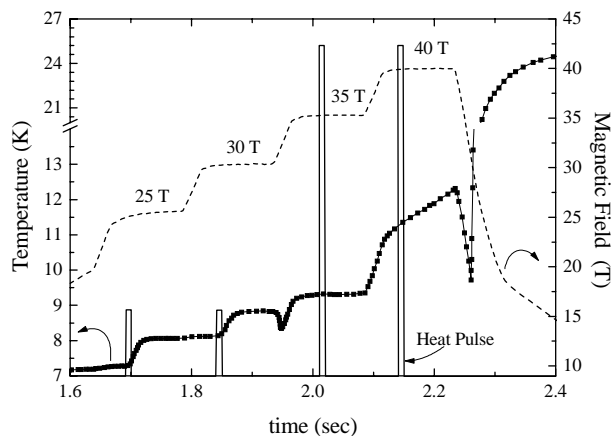


Figure 2. Staircase pulse shape for specific heat experiment on YbInCu₄. Dashed line – magnetic field. Solid line – voltage applied to the resistive heater. • - Thermometer's trace.

References:

- 1 Felner, I., *et al.*, Phys. Rev. B, **33**, 617 (1986).
- 2 Cornelius, A., *et al.*, Phys. Rev. B, **56**, 7993 (1997).
- 3 Sarrao, J.L., *et al.*, Phys. Rev. B, **58**, 409 (1998).
- 4 Immer, C.D., *et al.*, Phys. Rev. B, **56**, 71 (1997).

Magnetocaloric Effect Up to 60 T in Si, Ce₃Bi₄Pt₃ and UBe₁₃

NHMFL

Jaime, M., LANL

Movshovich, R., LANL

Sarrao, J.L., LANL

Canfield, P.C., Ames Laboratory, Iowa State Univ., Physics

Stewart, G.R., UF, Physics

The experimental study of physical properties in high magnetic fields has been demonstrated to be of great importance in solid state physics. The new Long Pulse 60 Tesla (LP 60 T) magnet, recently commissioned at the Los Alamos National Laboratory, produces a

flat-top field for a period of 100 ms at 60 T, and for longer time at lower fields. During the entire pulse, the magnetic field varies at a maximum ramp rate of $\partial B/\partial t \approx 400$ T/s. Together, these properties allow for the development of new tools to study materials in pulsed magnetic fields. Heat capacity and magnetocaloric effect (MCE) measurements are examples of these tools.

During the magnetic field sweep, the temperature of the stage does not stay constant even in the total absence of eddy current heating, due to the MCE.¹ The heat capacity stage, including sample, thermometer, and heater, is in thermal equilibrium, and under adiabatic condition during the magnetic field pulse.² Thus, the dependence of its temperature on the magnetic field during the pulse is then given by the expression

$$\left[\frac{\partial T}{\partial H} \right]_S = - \frac{T}{C_H} \left[\frac{\partial M}{\partial T} \right]_H \quad (1)$$

where T is temperature, H is magnetic field, M is magnetization, and C is the specific heat of the ensemble, and subscripts S and H indicate constant entropy and magnetic field, respectively. Equation 1 describes, for example, the process of adiabatic demagnetization cooling, where $[\partial M/\partial T]_H$ is negative, and $[\partial T/\partial H]_S$ is positive. Such a system warms as the field is increased, and cools when it is reduced, *reversibly*. Magnetization in general can also increase with temperature, in which case, the temperature of the sample shows the opposite behavior.

Examples of the MCE measured with our plastic calorimeter are displayed in Figure 1, for the 10 mg Si platform, Figure 2 for a 111.5 mg sample of $\text{Ce}_3\text{Bi}_4\text{Pt}_3$, and Figure 3 for a 4.3 mg sample of UBe_{13} . The latter one was measured in two different ways, with a 303 mg Si block glued to the platform and without it. The MCE is relatively small for the Si platform, and includes the MCE intrinsic to thermometer and heater. The effect in $\text{Ce}_3\text{Bi}_4\text{Pt}_3$ is overall negative, with a low field positive contribution that grows at low temperatures. The negative MCE is consistent with $[\partial M/\partial T]_H > 0$ observed in this material below 80

K, at high fields.³ The positive MCE at low fields is likely an indication of magnetic impurities. The low temperature traces show an anomaly at $H \approx 50$ T, which may indicate transition into a phase with different spin dynamics. UBe_{13} , on the other hand, shows a large positive MCE. Attempts

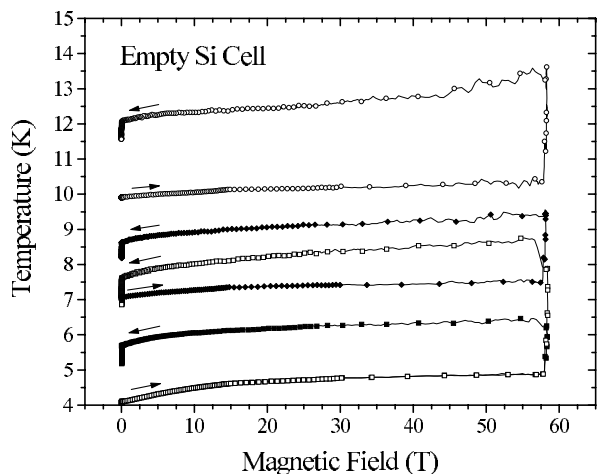


Figure 1. Temperature vs. magnetic field for the heat capacity stage (10 mg Si platform + Cernox thermometer + chip resistor). For each of the traces the temperature increases slightly during the field up-sweep. During the field plateau at 60 T, the delivery of heat pulses causes the temperature to increase. The temperature decreases consistently during the field down-sweep. If no heat pulses are delivered at the plateau, not shown, the temperature variation during the field cycle is reversible.

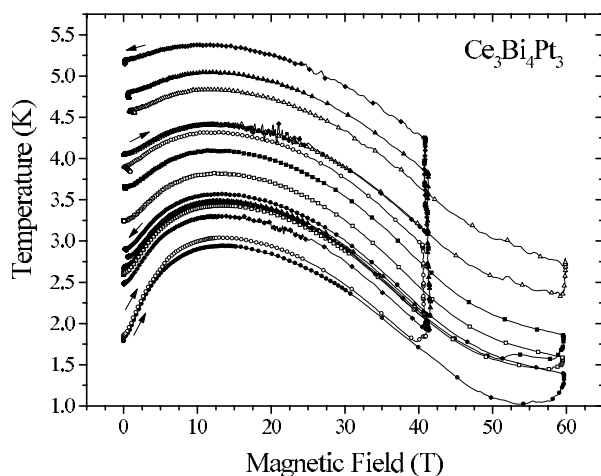


Figure 2. Temperature vs. magnetic field for a sample of $\text{Ce}_3\text{Bi}_4\text{Pt}_3$ (111.5 mg). Several 40 T and 60 T magnetic field pulses are displayed, with delivery of heat at the plateau. The open squares correspond to a temperature trace when heat was not delivered to the sample. Some irreversibility in the temperature is observed for this sample.

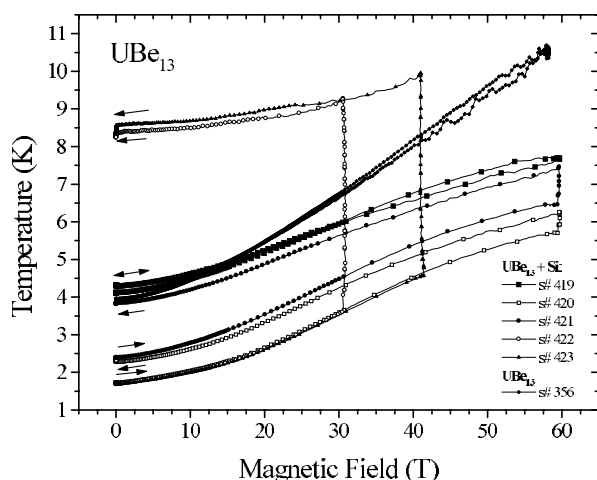


Figure 3. Temperature vs. magnetic field for a sample of UBe_{13} (4.3 mg), with and without a 303 mg Si single crystal glued to the heat capacity stage. Solid squares and solid diamonds correspond to experiments where no heat pulses are delivered to the sample during the field plateau, and illustrate the reversibility of the stage's temperature during the field cycle.

were made to reduce the magnitude of the temperature increase in the magnetic field by gluing a piece of single crystal Si to the platform. Figure 3 shows how the Si lattice helps to reduce the temperature increase by a factor of two. Such a big MCE in UBe_{13} indicates that the heat capacity of the material at low temperatures must be strongly reduced by a magnetic field of 60 T.

References:

- 1 Hudson, R.P., Principles and Applications of Magnetic Cooling (1972).
- 2 See Jaime, M., *et al.*, elsewhere in this volume.
- 3 Modler, R., *et al.*, to be published.

De Haas van Alphen Experiments in YbXCu_4 and LuXCu_4

Lawrence, J.M., Univ. of California–Irvine, Physics and Astronomy
Cornelius, A.L., LANL

The compounds YbXCu_4 grow in the cubic C15b structure for a number of elements $X = \text{Ag, Au, Cd, In, Mg, Tl, Zn}$. High quality single crystals

can be grown from relatively low temperature fluxes. The compounds exhibit a variety of ground states: antiferromagnetic, heavy fermion and strongly mixed-valent. The Kondo temperatures span the range from 1-1000 K. These compounds offer an excellent opportunity to explore the behavior of the heavy fermion/mixed valent ground state over a broad range of valences and Kondo temperatures. We have begun¹ experiments with the intent of carrying out a systematic comparison of the susceptibility $\chi(T)$, specific heat coefficient γ , Yb 4f hole occupation number $n_f(T)$ (measured by L_3 x-ray absorption) and the dynamic susceptibility $\chi''(\omega)$ (measured by inelastic neutron scattering) to the predictions of the Anderson impurity theory. By comparing the data for such a large series of related compounds, and with such a broad spread of Kondo temperatures to calculations performed simultaneously for several experimental quantities, we hope to provide a test of the applicability of the model that is both stringent and unique.

There are two good reasons for measuring the de Haas van Alphen (dHvA) effect in these samples. (1) In performing calculations for the Anderson model, there are essentially three input parameters: the distance $\Delta E_f = E_f - \epsilon_F$ of the 4f level energy E_f from the Fermi level ϵ_F , the background bandwidth D and the 4f/conduction electron hybridization element V . These are typically chosen so as to replicate as well as possible the behavior of $\chi(T)$ and $n_f(T)$. Recently it has become possible to calculate these parameters from first principles, using a combination of LDA and many-body theory.² Knowledge of the background bandstructure through dHvA in the LuXCu_4 compounds would be valuable input to such a theoretical program, and would add a strong additional constraint on the effort comparing the experimental results to the Anderson model predictions. (2) One of the key manifestations of coherence is that the Kondo interactions give rise to a renormalized bandstructure; typically the topology of the Fermi level is unaffected, but the bands take on large effective masses. This renormalized band structure is best measured via dHvA experiments in the YbXCu_4 compounds.

In September, we made an initial effort to determine the dHvA signals in YbInCu₄, YbAgCu₄, LuInCu₄ and LuAgCu₄. These attempts were not successful for two reasons: (1) the crystal quality (as measured by the resistance ratio or RRR) was inadequate; and (2) we used a probe that appeared to have an induced mechanical vibration in the presence of the pulsed field; this vibration gave a signal that was periodic in time, which complicated the analysis.

Our current plan is to bring a postdoc to Los Alamos for an extended period to solve these problems. We will work with John Sarrao of MST-10 to ensure that the samples we use for the dHvA measurement are of the highest possible quality. Second, Cornelius is rewinding the coil on his probe (the coil had broken just prior to the September run); this probe does not suffer from the mechanical vibration, so we will use it in future runs.

References:

- 1 Sarrao, J.L., *et al.*, Phys. Rev. B., to be published.
- 2 Han, J.E., *et al.*, Phys. Rev. Lett, **78**, 939 (1997).

SmB₆ in Megagauss Fields

Mielke, C.H., NHMFL/LANL
 Cooley, J.C., LANL
 Smith, J.L., LANL
 Goettee, J.D., NHMFL/LANL
 Honold, M., Oxford Univ., Physics
 Dominguez, T., NHMFL/LANL
 Pacheco, M., NHMFL/LANL
 Bowman, W., NHMFL/LANL
 Roybal, S., NHMFL/LANL
 Bennett, M., NHMFL/LANL
 Betts, J., NHMFL/LANL
 King, J., NHMFL/LANL
 Herrera, D., NHMFL/LANL
 Torres, D., NHMFL/LANL
 Rickel, D.G., NHMFL/LANL
 Lacerda, A.H., NHMFL/LANL

The magnetotransport of SmB₆ to fields of 145 T at a temperature of ~8 K was reported in the 1997 NHMFL Annual Report.¹ As we indicated further measurements have been performed to verify the

earlier results. Figure 1 shows the results reported last year as well as the more recent flux compression results. Magnetotransport results measured in a 60 T non-destructive magnet are shown as a dashed line. Good agreement between the non-destructive shot and the flux compression data are observed. At this time an explanation for the strong positive magnetoresistance above the $\rho(H)$ minima are still being developed.

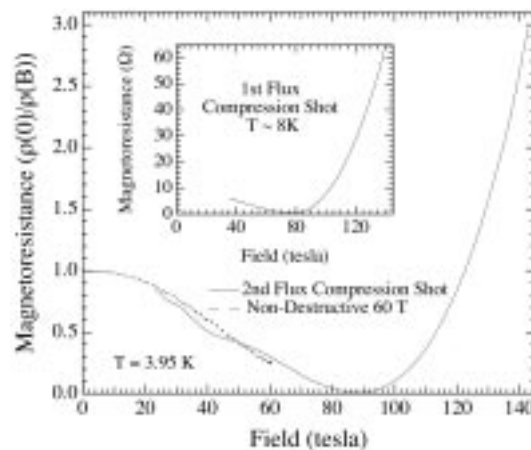


Figure 1. The magnetotransport of SmB₆ measured to 145 T. The inset shows earlier results.¹ The dashed line are results from a non-destructive pulsed magnet.

Reference:

- 1 Mielke, C.H., *et al.*, NHMFL Annual Report, **1**, 88 (1997).

Pressure Effect on the Metamagnetic Transition of UNiAl

Mikulina, O., Academy of Sciences-Czech Republic, Institute of Physics
 Lacerda, A.H., NHMFL/LANL
 Kamarad, J., Academy of Sciences-Czech Republic, Institute of Physics
 Syshchenko, A., Charles Univ.-Czech Republic, Metal Physics
 Sechovsky, V., Charles Univ.-Czech Republic, Metal Physics
 Nakotte, H., New Mexico State Univ.-Las Cruces, Physics
 Beyermann, W.P., Univ. of California-Irvine, Physics

We have investigated the effect of pressure and magnetic field on the metamagnetic transition of

UNiAl single crystal. UNiAl crystallizes in the hexagonal ZrNiAl-type structure and orders antiferromagnetically (AF) below $T_N = 19.3$ K. Transverse magnetoresistance was measured with the current along the a-axis, and the magnetic field along the c-axis of the hexagonal structure. A clear decrease of scattering is noticed at the metamagnetic transition at all temperatures investigated. At temperatures below 6 K the magnetoresistance drop becomes very sharp, and may indicate features of a first order transition.

We have measured resistivity under pressure (up to 10 kbar) to 200 K, and magnetoresistance to 18 T at different temperatures and pressures. Figure 1 shows the transverse magnetoresistance at 8 kbar, and different applied magnetic fields. A drastic change in the scattering mechanism is observed at around the metamagnetic transition (11.5 T). Hysteresis is observed at low pressure in the low temperature magnetoresistance measurements as the sample is zero field cooled or in field cooled. This behavior, in addition to recent Neutron Scattering measurements, suggests that a new AF structure with a different propagation vector emerges at low temperature.

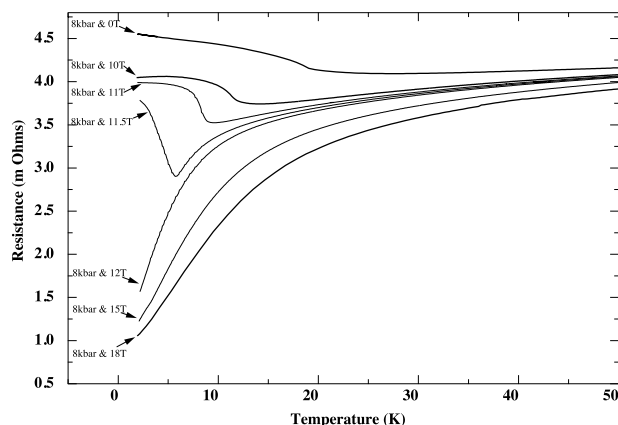


Figure 1. Resistance versus temperature of UNiAl at 8 kbar and applied magnetic fields.

This work is supported by the NSF-Division of International Programs.

Magnetization Measurements of Correlated Electron Systems

Modler, R., LANL
 Thompson, J.D., LANL
 Sarrao, J.L., LANL
 Torelli, M.E., NHMFL/FSU, Physics
 Fisk, Z., NHMFL

We investigated the isothermal magnetization of powder samples of four different material classes: (1) CeRh_2Si_2 and (2) $\text{Ce}_3\text{Bi}_4\text{Pt}_3$, as well as, various doping series around “base stoichiometries” (3) MnSi and (4) YbInCu₄. Magnetization was measured using a standard extraction method in the short-pulse magnets located at Los Alamos National Laboratory. Data has been taken in a temperature range from 1.5 K to 250 K, and magnetic fields up to 60 T. We emphasized the low temperature measurements (1.5 K to 4 K), which provide valuable information regarding the ground states of the various systems.

(1) From our magnetization measurements on the antiferromagnet kondo lattice CeRh_2Si_2 , we obtained detailed information about a high-field magnetic phase transition. The data allowed the construction of the magnetic B-T phase diagram of CeRh_2Si_2 , which turns out to be very similar to the one associated with the isostructural heavy-fermion superconductor CeCu_2Si_2 . A simple energy scaling reveals the scaling of the magnetic phase diagrams of both compounds with regard to the size of the magnetic moment involved in the magnetic ordering.¹

(2) High field magnetization results up to 60 T on the Kondo insulator $\text{Ce}_3\text{Bi}_4\text{Pt}_3$ show that the residual ($T=0$) susceptibility in the insulating state is in fact an intrinsic property of the material. (any impurities would be saturated in a magnetic field of this magnitude). The remaining $T=0$ susceptibility could be understood as a van Vleck-like susceptibility which is associated with the polarization of the local Kondo singlets. Unlike earlier high-field transport measurements on $\text{Ce}_3\text{Bi}_4\text{Pt}_3$, would suggest² however, the magnetization appears to be linear up to magnetic fields of 60 T, which indicates that the hybridization

gap is robust against fields of this magnitude. We interpret this discrepancy to transport investigations as a possible result of a small anisotropy of the hybridization gap.

(3) We have also studied the field-induced valence transition in YbInCu_4 and doped variants (e.g. $\text{Yb}_{1-x}\text{Y}_x\text{InCu}_4$ and $\text{YbIn}_{1-x}\text{Ag}_x\text{Cu}_4$). Remarkably, despite the introduction of either f -site or ligand-disorder, a universal scaling behavior of the B - T phase diagrams is observed once the data are properly scaled. In a related set of materials, Yb_xCu_4 (where X is a semi-metal or late transition metal), we have examined the validity of the single-impurity Anderson model in describing the magnetic response of dense Kondo systems by comparing our magnetization data with theoretical predictions.

(4) Further, we have started a study of the response of the well-known helimagnetism in MnSi to doping and magnetic field, in search for non-Fermi liquid behavior in these materials.

References:

- 1 Modler, R., *et al.*, Proceedings of the International Conference on Physical Phenomena in High Magnetic Fields, Tallahassee, FL, October 24-27, 1998.
- 2 Boebinger, G., *et al.*, Physica B, **211**, 227 (1995).

Ultrasonic Velocity Measurements in UPt_3 at the Metamagnetic Transition

Sarma, B.K., Univ. of Wisconsin at Milwaukee, Physics
 Feller, J., Univ. of Wisconsin at Milwaukee, Physics
 Ketterson, J.B., Northwestern Univ., Physics

Instrumentation to do ultrasonic studies of strongly correlated electron systems in very high magnetic fields is being developed. Ultrasonic velocity and attenuation measurements have been performed on UPt_3 at high magnetic fields at the NHMFL in Tallahassee. The experiments were done during two separate runs during 1998. Measurements were performed on the 30 T resistive magnet in cell 9

using both ^4He and ^3He cryostats, and also in the dilution refrigerator with the 20 T superconducting magnet.

UPt_3 shows metamagnetic behavior at a field of 20.3 T, where over a narrow field range the velocity (elastic constant) shows a pronounced dip (softening). The change in velocity is about 2% at 2 K, and higher at lower temperatures. In this range the magnetization shows a step increase (the magnetic susceptibility showing a peak). For the first time it was possible to measure the dispersion in the velocity (frequency dependence) at this transition (Figure 1). When measurements were extended to lower temperatures (^3He insert and the dilution refrigerator), the transition became sharper (the velocity dip larger) and a new shoulder appears in the high field side of the transition (Figure 2).

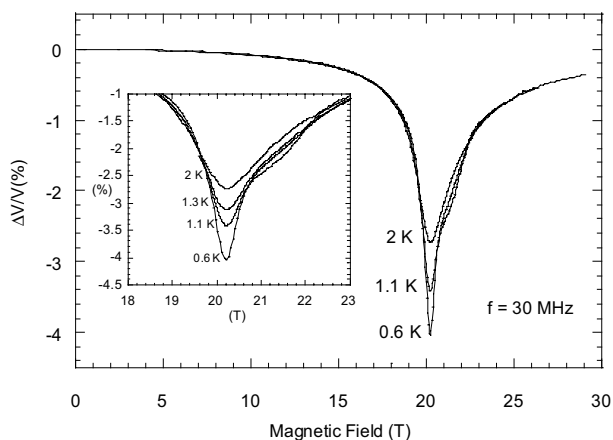


Figure 1. Velocity change at the metamagnetic transition in UPt_3 . The inset shows the dispersion.

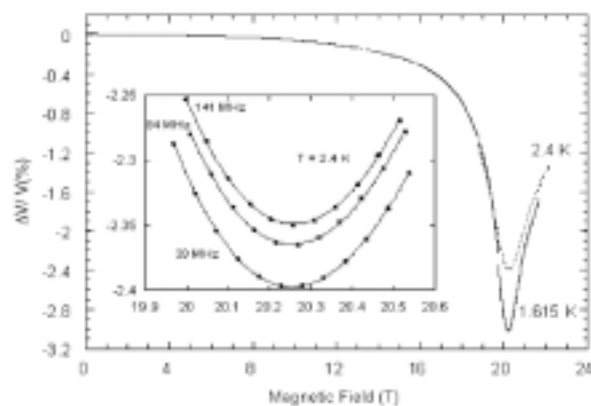


Figure 2. Additional features are seen in the velocity at lower temperatures.

Magnetostriction and Thermal Expansion of UBe_{13}

Schmiedeshoff, G.M., Occidental College, Physics
Lacerda, A.H., NHMFL/LANL
Smith, J.L., LANL

We have measured the thermal expansion of a 4 mm long cylinder of polycrystalline UBe_{13} to 2 K and in magnetic fields to 18 T. We have also measured the magnetostriction of this sample of UBe_{13} to 18 T at 10 K. Both measurements were made with an OFHC copper dilatometer now available to users at the NHMFL-Los Alamos. The thermal expansion exhibits a broad minimum centered near 12 K in agreement with earlier measurements.² This minimum is thought to be associated with the onset of the coherent heavy fermion state in this material. We find this temperature dependence (of the thermal expansion) to be independent of field to 18 T within experimental resolution. The magnetostriction at 10 K exhibits a clear H^2 dependence as expected for a paramagnetic metal, this result is also consistent with earlier measurements.

References:

- 1 Lacerda, A., *et al.*, Phys. Rev. B, **40**, 11429 (1989).
- 2 de Visser, A., *et al.*, Phys. Rev. B, **45**, 962 (1992).

Quantum Acoustic Oscillations in UPt_3

Shivaram, B.S., Univ. of Virginia, Physics
Ulrich, V., Univ. of Virginia, Physics
Hinks, D.G., Argonne National Laboratories

We have used the new 33 T mK facility at NHMFL, Tallahassee, as well as the 20 T SCM-1 system to perform high resolution longitudinal ultrasound velocity measurements in the heavy electron material UPt_3 down to temperatures of 35 mK. The measurements were performed on the same high

quality single crystal used in earlier high pressure phase diagram studies.¹ Measurements were taken at several orientations of the field with respect to the crystal axes. This was achieved in the case of SCM-1 with the rotator, and in the case of the 33 T magnet by means of specially designed wedges. The probe in the 33 T system also had to be outfitted with low loss coaxial lines in order to obtain reliable signals. This turned out to be the key to obtaining the high quality of results shown here. A similar modification for the SCM-1 will go a long way in improving future results from ultrasound experiments.

Figure 1 shows the change in the sound velocity results obtained for two orthogonal orientations of the field, B. In the upper part is shown quantum oscillations in the sound velocity for B // a-axis, which first appear at roughly 13 T. These oscillations correspond to the 'Γ-orbit' with a frequency of 7.4 Mg, which shows up in band structure calculations.² These oscillations undergo dramatic changes in frequency near B = 20 T, where there is a metamagnetic transition. When the oscillations reemerge on the upper side of the transition they have a completely different frequency.

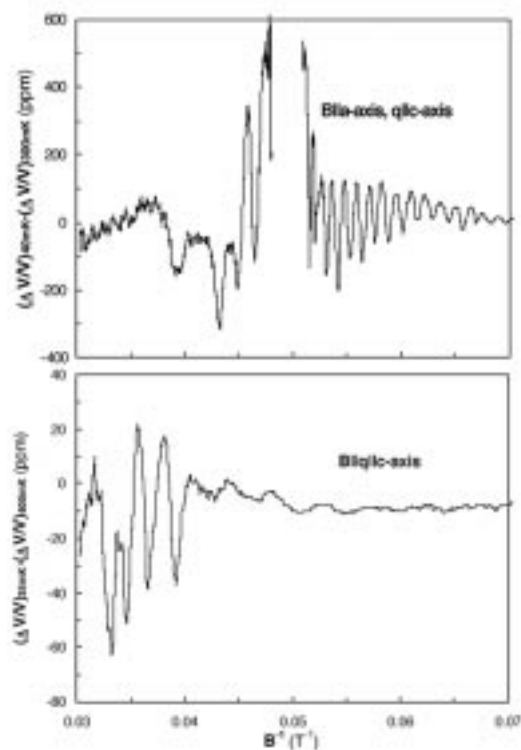


Figure 1. Shows changes in the sound velocity in UPt_3 for B//a-axis (top) and B//c-axis (bottom).

The lower part of the figure shows the quantum oscillations for $B // c$ -axis. Apart from the very recent work from Japan³ this is the first observation of Fermi surface related oscillations in this direction. Here again we observe new effects—there is a sudden increase in the amplitude of the oscillations around 24 T accompanied by a rapid increase in the frequency reminiscent of the behavior for $B // a$ -axis below the meta-magnetic transition. This could mean there is a further rearrangement of the Fermi surface in higher fields.

References:

- 1 Boukhny, M., *et al.*, Phys. Rev. Lett., **73**, 1707 (1994).
- 2 Norman, M.R., *et al.*, Solid St. Comm., **68**, 245 1988.
- 3 Kimura, N., *et al.*, J. Phys. Soc. Japan, **67**, 2185 (1998).

Measurement of the Specific Heat of Two Highly Correlated Heavy Fermion Systems (UBe_{13} and $U_{0.97}Th_{0.03}Be_{13}$) in Pulsed Fields to 60 T

Stewart, G.R., UF, Physics/NHMFL
 Kim, J.S., UF, Physics
 Movshovich, R., LANL/NHMFL
 Jaime, M., LANL/NHMFL

Among the heavy fermion systems whose variation of the specific heat with high applied magnetic field is known,¹ UBe_{13} is the exception with a very small change of γ ($\equiv C/T$ as $T \rightarrow 0$) ($< \sim 5\%$) in 20 T. The γ in $U_{0.97}Th_{0.03}Be_{13}$ is twice that as in UBe_{13} , and therefore the characteristic energy ($T_K \propto 1/\gamma$) for the thorium doped compound is only half that of the pure UBe_{13} . A simple phenomenological argument would then infer that the field dependence of γ in $U_{0.97}Th_{0.03}Be_{13}$ in high field should be twice that of UBe_{13} .

After first confirming the small change of γ in UBe_{13} in 30 T at NHMFL in Tallahassee, we have carried out pulsed field specific heat experiments in the new long pulse calorimeter² at LANL/

NHMFL up to 60 T on both compounds. Results of the data analysis will be forthcoming soon.

References:

- 1 Andraka, B., *et al.*, Phys. Rev. B, **39**, 6420 (1989).
- 2 Jaime, M., *et al.*, to appear in the proceedings of the PPHMF-III Conference, October 24-27, 1998, Tallahassee, FL.

Scaling of the Magnetization in Magnetic Fields to 30 T of $UCu_{5-x}Pd_x$: Evidence for a Crossover from Correlated to Single Ion Magnetic Interactions Upon Cooling

Stewart, G.R., UF, Physics/NHMFL
 Kim, J.S., UF, Physics
 Thomas, S., UF, Physics
 Hall, D., NHMFL

Scaling of low temperature magnetization data for the non-Fermi liquid systems UCu_4Pd and $UCu_{3.5}Pd_{1.5}$ in fields to 30 T was carried out to help determine the nature of the magnetic interactions above and below 10 K. The size of the scaling exponent, β , found from this scaling with field above 10 K implies that the higher temperature magnetic excitations in UCu_4Pd are correlated, i.e. $\beta > 1.0$. For $T \leq 6K$, $\beta < 1.0$ for both compounds implying that the interactions may change and assume single-ion character, consistent with recent doping experiments. These results contradict a recent neutron scattering study¹ and may be understood theoretically as a depletion of the occupation of the phase space of magnetic excitations with decreasing temperature (\Leftrightarrow energy), leading to a decoupling of the excitations.

Reference:

- 1 Aronson, M.C., *et al.*, J. Phys.: Condens. Matter, **8**, 9815 (1996).

Magnetic Phase Transitions in UNiGe Under Pressure

Syshchenko, A., Charles Univ., The Czech Republic,
Dept. of Metal Physics

Sechovsky, V., Charles Univ., The Czech Republic, Dept.
of Metal Physics

Mikulina, O., Institute of Physics, Academy of Sciences,
The Czech Republic

Kamarad, J., Institute of Physics, Academy of Sciences,
The Czech Republic

Lacerda, A.H., NHMFL/LANL

Nakotte, H., New Mexico State Univ.-Las Cruces, Physics

Beyermann, W.P., Univ. of California-Irvine, Physics

Under the auspices of the National Science Foundation Division of International Programs, we have built and tested a high pressure cell to be utilized in the 20 T superconducting magnet at the NHMFL-LANL Facility. We are now in the process of building a non-magnet cell to be used in the 60 T Long Pulse magnet. The following is a short description of the first measurement.

UNiGe orders antiferromagnetically at $T_N = 50$ K in an incommensurate spin density wave with $q = (0, \delta, \delta)$, $\delta \approx 0.35$ and undergoes a first order magnetic phase transition at $T_1 = 41.5$ K to a commensurate low-temperature magnetic phase with $q = (0, 1/2, 1/2)$.¹ The electrical resistivity with current along the *c*-axis² weakly increases with decreasing temperature from room temperature down to T_N . This trend is gradually suppressed below T_N until a small, but visible, negative step on the $\rho(T)$ curve is observed at T_1 and followed by a precipitous decrease of the resistivity with further decreasing temperature. In magnetic fields applied along the *c*-axis, the ground-state is transformed toward the ferromagnetic alignment of U moments in two steps by metamagnetic transitions at ≈ 3 and 10 T, at 4.2 K.³ These transitions are accompanied by GMR effects.

Our experiment focused on the influence of external hydrostatic pressure on the electrical resistivity of a UNiGe single crystal (with current along the *c* axis) as a function of temperature, magnetic field, and external hydrostatic pressure.

Figure 1 shows data from the present experiment in zero field, namely the temperature dependence of the electrical resistivity of UNiGe at ambient pressure and 6.5 kbar. Longitudinal magnetoresistivity curves measured in fields applied along the *c*-axis on UNiGe under ambient pressure and pressures of 2 kbar and 6.5 kbar are shown in Figure 2.

Analysis of relevant resistivity and magnetoresistance anomalies allows us to determine pressure induced changes of critical temperatures and magnetic fields of magnetic phase transitions in this material. The observed results reflect pressure induced changes of interatomic distances and consequent variations of exchange interactions.

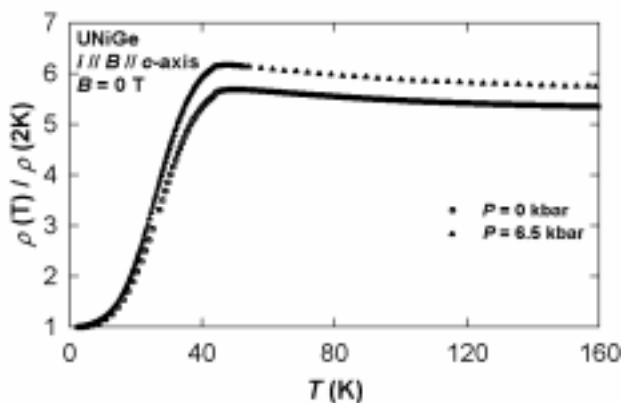


Figure 1. R vs. T at 0 and 6.5 kbar.

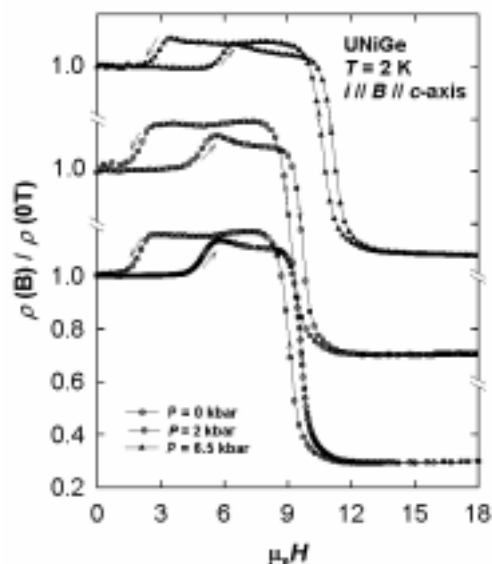


Figure 2. Magnetoresistance at different pressures at 2 K.

This work is supported by the NSF Division of International Programs.

References:

- 1 Nakotte, H., *et al.*, Phys. Rev. B, **54**, 7201 (1996).
- 2 Prokes, K., *et al.*, IEEE Trans. Magn., **30**, 1214 (1994).
- 3 Havela, L., *et al.*, Physica B, **177**, 159 (1992).

Magnetotransport Studies of CeP

Terashima, T., Tsukuba Magnet Laboratory, National Research Institute for Metals (NRIM)

Uji, S., Tsukuba Magnet Laboratory, NRIM

Aoki, H., Tsukuba Magnet Laboratory, NRIM

Qualls, J.S., NHMFL

Stalcup, T.F., NHMFL

Brooks, J.S., NHMFL/FSU, Physics

Haga, Y., Advanced Science Research Center, Japan

Atomic Energy Research Institute

Uesawa, A., Tohoku Univ., Physics

Suzuki, T., Tohoku Univ., Physics

CeP is a low-carrier-density compensated semimetal, in which electron and hole carriers originate from Ce $5d$ and P $3p$ states, respectively. It is also a magnetic compound consisting of Ce $4f$ localized moments. The interplay between those two subsystems underlies various unusual transport and magnetic properties which CeP exhibits.¹ We have been studying this compound through magnetotransport measurements. The primary results obtained so far are as follows.

CeP have two major magnetic transition temperatures, T_H and T_L , at low fields.¹ Ferromagnetic layers appear periodically in a sea of paramagnetic layers at T_H , while the remaining paramagnetic layers order antiferromagnetically at T_L . On the other hand, CeP has been believed to be a simple antiferromagnet at zero magnetic field. The T_H transition in field is accompanied by a large drop in resistivity. A magnetic polaron model has been proposed to account for that.² Its essential

assumption is that magnetic polarons existing as droplets in the paramagnetic state act as effective scattering centers. They form a lattice, i.e. periodically stacked ferromagnetic layers, at the T_H transition, which results in reduction of resistivity. A puzzle here is that a substantial resistivity drop is also observed at the zero-field “antiferromagnetic” order. This motivated us to carry out resistivity vs. temperature measurements at zero and low fields. What we found is that CeP has two magnetic transitions even at zero field; one is a second-order transition characterized by critical scattering, presumed to be an antiferromagnetic order, while the other is of first order, most likely corresponding to appearance of the ferromagnetic layers.

CeP shows numerous successive metamagnetic transitions by application of high field.³ Last year, we made longitudinal magnetoresistance measurements for the magnetic field parallel to [001] and determined the phase diagram for this field direction,⁴ which turned out to show considerable disagreement with a previously reported one. As an extension of this, we have performed angular study this year by measuring transverse magnetoresistance for field directions tilted from [001]. Phase diagrams for different field directions look surprisingly similar when

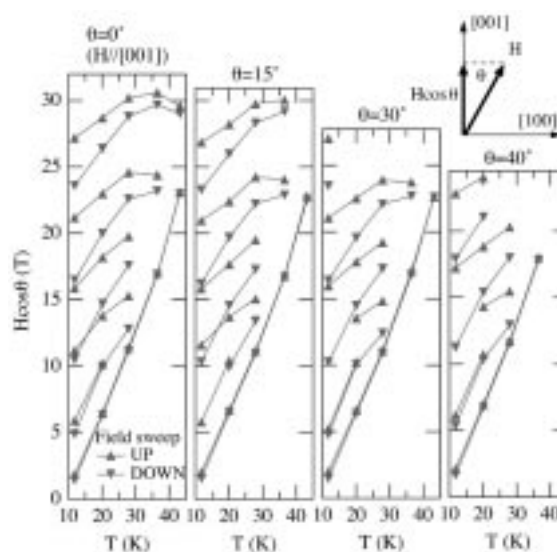


Figure 1. Magnetic phase diagrams of CeP for different field directions. The vertical axis $H\cos\theta$ corresponds to the [001] component of the field.

the [001] component of the field is chosen as a vertical axis (Figure 1). This extreme uniaxial anisotropy indicates that the p - f mixing interaction which was proposed by Kasuya to explain anomalous properties of CeSb is also operative in CeP.²

Hall measurements up to 26 T were made and the data is being analyzed.

References:

- 1 Suzuki, T., *et al.*, Physica B, **206 & 207**, 771 (1995).
- 2 Kasuya, T., *et al.*, J. Phys. Soc. Jpn., **62**, 3376 (1993) and references therein.
- 3 Kuroda, T., *et al.*, Physica B, **186-188**, 396 (1993).
- 4 Terashima, T., *et al.*, Phys. Rev. B, **58**, 309 (1998).

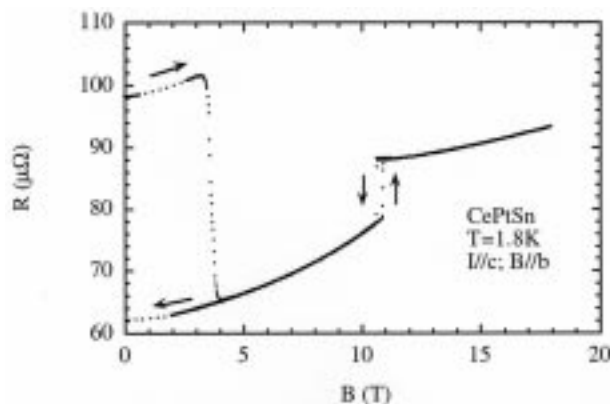
Magnetic Properties of the Kondo Lattice Compound CePtSn

Torikachvili, M. S., San Diego State Univ., Physics
 Nakotte, H., New Mexico State Univ., Physics
 Takabatake, A., Hiroshima Univ.

The Kondo lattice compound CePtSn orders antiferromagnetically with $T_N \approx 7.5$ K. A second magnetic transition can be observed at $T_M \approx 4.8$ K. The crystal structure is orthorhombic, the electronic and magnetic properties are quite anisotropic, and the easy direction of magnetization is the a-axis. The magnetic structure, as determined from neutron scattering measurements, is quite complex.¹

In order to probe the magnetic phase diagram of CePtSn, we performed measurements of magnetization (M) and magnetoresistance (MR) in $B \leq 18$ T in a single crystal, at the NHMFL-Los Alamos. The M vs. B data for B//a-axis at 2 K shows a positive curvature from 8 to 12 T, while the M vs. B data at 2 K for B//b-axis shows a step increase at 10.5 T. Both these features are suggestive of spin reorientation. The electrical resistivity shows a minimum at 25 K, a

maximum at 8 K, followed by a sharp drop below T_N , and a change of slope at T_M . Curves of R vs. T in $B \leq 18$ T, with B//a- or b-axis, show that the feature at T_N moves to lower T with B, eventually disappearing at higher B. The MR at 1.8 K for B//a-axis is positive, and it shows two reversible features; a sharp, large drop at 12.5 T, and a small drop at 17.5 T. Both these features are suggestive of spin realignment. The R vs. B data for B//b-axis at 1.8 K displays a sharp drop at 3.5 T, and a sharp increase at 11 T, as shown in Figure 1. While the feature at 11 T is reversible and correlates well in field with the transition observed in the M vs. B data, the transition at 3.5 T is not reversible, suggesting that the spin realigned phase is metastable.



Reference:

- 1 Kadowaki, H., *et al.*, J. Phys. Soc. Japan, **12**, 4426 (1993).